A Discrete Reeb Graph Approach for the Segmentation of Human Body Scans

Yijun Xiao, Paul Siebert
Department of Computing Sciences
University of Glasgow
{yjxiao, psiebert}@dcs.gla.ac.uk

Naoufel Werghi
College of Information Technology
Dubai University College
nwerghi@duc.ac.ae

Abstract

Segmentation of 3D human body (HB) scan is a very challenging problem in applications exploiting human scan data. To tackle this problem, this paper proposes a topological approach based on Discrete Reeb Graph (DRG) which is an extension of the classical Reeb Graph to unorganized cloud of 3D points. The essence of the approach is detecting critical nodes in the DRG thus permitting the extraction of branches that represent the body parts. Because the human body shape representation is built upon global topological features that are preserved so long as the whole structure of the human body does not change, our approach is quite robust against noise, holes, irregular sampling, moderate reference change and posture variation. Experimental results performed on real scan data demonstrate the validity of our method.

1 Introduction

The recent years have seen the emergence of 3D imaging technology that enables full scanning of the HB surface with reasonable measurement accuracy and acceptable computational cost. This advance facilitates the exploitation of the HB form in various areas such as anthropometrical research [1, 2, 18], clothing design [3, 4, 5] and virtual human animation [6]. Although the raw data delivered by the HB scanner requires substantial main memory and backing store resources, this data contains little semantic information. For the effective and efficient use of body scan data, it is usually necessary to partition the whole scan data set into subsets corresponding to the different principal body parts. This segmentation provides the basis for a high-level representation of the scan data and is a prerequisite for further semantic analysis. For example, in medical applications, the segmentation process provides an atlas for extracting data belonging to limbs that can be used to guide further analysis such as fitting generic limb models. These models can then be used to automate specific clinical protocols, such as spinal curvature assessment. Applications dealing with human body motion estimation from range images data [7] can exploit the scan data segmentation in initializing the parameters of the tracking algorithm. HB scan segmentation is also useful for the online garment shopping [4, 5] as it can contribute in providing accurate body measurement and sizing.

Automatic segmentation of HB data is a challenging problem firstly because the body shape is both articulated and deformable and secondly because the scan data by nature is non-uniformly sampled, often containing gaps and corrupted by measurement noise.

The automatic segmentation of the HB scan data into the functional parts was pioneered by Nurre [8]. He approximated the body structure by a stick-template representing the head, the two arms, the two legs and the torso. His goal was to segment the body into six segments corresponding to these parts. This approach combines a global shape description, namely moments analysis, and local criteria of proximity which are derived from a priori knowledge of the relative positions of the body parts in the standard posture (standing body with arms held at the sides). The range data is organized into slices of data points. The horizontal slices are stacked vertically and the data points are assigned to the different body parts according to the slice's topology and its position in the body. E.g. a slice having two separated closed curves must represent data points measured at the level of the legs. A slice consisting of three closed curves must belong to the torso and arms area, a slice with two joined closed curves is assumed to correspond to the transition between the legs and the torso (at the level of the groin). Certainly this work illustrated a considerable progress towards the automatic decomposition of the HB data, however the approach is restricted to a strict standard posture and did not show evidence of robustness with respect to noise, gaps in the data, and variation in the shape and the posture of the HB.

Using the framework of Nurre, Ju *et al* [9] refined this segmentation approach by introducing curvature analysis of profiles extracted from the slices to allow further decom-

Proceedings of the Fourth International Conference on 3-D Digital Imaging and Modeling (3DIM'03)
0-7695-1991-1/03 $ 17.00 © 2003 IEEE

position of the body limbs into their articulated segments. Decker and Douros *et al* [10, 11] advanced Nurre's work by improving the localization of the key landmarks of HB. For instance, they differentiated the slice circumferences in the torso area to locate the waist position. However their approach had the same limitations of Nurre's approach [8]. Recently, Wang et al[9] proposed an approach developed within a Fuzzy logic framework. As with Nurre's approach, a strict standing posture is assumed. After many preparation stages, the data is meshed and a segmentation technique applied that involves local curvature analysis of the slice data. However the overall performance of this approach remains identical to that of Nurre's.

In conclusion, the approaches developed to date are restricted by their underlying assumptions and may well suffer from instability when applied to real applications that must process noisy and corrupted 3D HB scan data containing posture variations. Furthermore, no evidence of the repeatability of these previous algorithms has been reported in the literature. For a HB data segmentation to be of practical utility, it must be robust to the variations of the body surface shape stemming from biological factors such as age, genetics, etc. It must also cope with reasonable perturbations in body posture. *Adhoc* techniques cannot satisfy these requirements, although they might work for a particular case. This paper proposes an approach defined within a general topological analysis framework. A systematic way to segment HB body data is presented that can cope with body shape variations and moderate posture changes. The approach does not require any pre-processing stages, operates on raw 3D point-cloud data and does not involve local feature analysis, which would be vulnerable to deficiencies in the scan data.

The rest of the paper is organized as follows: Section 2 describes the theoretical foundation of the approach and its relation with Morse theory and the Reed Graph. Section 3 describes the segmentation algorithm. The experiments and their results are presented in Section 4. The paper concludes in section 5 with a discussion of the results and future work.

2 Morse Theory and Reeb Graph

Morse theory can be thought of as a generalization of the classical theory of critical points (maxima, minima and saddle points) of smooth functions on Euclidean spaces. Morse theory states that for a generic function defined on a closed compact manifold (e.g. a closed surface) the nature of its critical points determines the topology of the manifold. Morse functions are generic functions for which all the critical points are non-degenerate (Hessian matrix of the function at the critical point is non singular). For a Morse function, the critical points determines the homology groups of the manifold, that is a sets of points for which

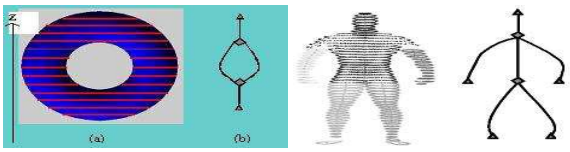

(c)

Figure 1. Reeb graph of a torus,Reeb graph of a human figure.

the function is less than a given value. Moreover these sets can fully describe the topology of the manifold. The way the manifold is embedded in the 3D space can be coded using the Reeb graph which is a skeleton graph that encodes the evolution and the arrangement of the homology groups. Reeb graph represents the configuration of critical points and their relationship and provides a way to understand the intrinsic topological structure of a shape. Reeb graph has been used in many applications such as shape matching [13] , shape coding [14] and surface description and compression [15, 16]. A Reeb graph is defined as follows:

Definition1*: Let* **f** *be a real-valued function on a compact manifold M. The Reeb graph of* **f** *is the quotient space of the graph of* **f** *in M by the equivalence relation* " $\sim$ " *defined by* $(X_1, f(X_1)) \sim (X_2, \boldsymbol{f}(X_2))$ *if* $\boldsymbol{f}(X_1) = \boldsymbol{f}(X_2)$ *and* X_1 *and* X_2 *are in the same connected component of* $\boldsymbol{f}^{-1}((\boldsymbol{f}(X_1))$.

Roughly speaking, the two pairs $(X_1, f(X_1))$ and $(X_2, f(X_2))$ are represented as the same element in the Reeb graph if the values of f are the same and if they belong to the same connected component of the inverse image of $f(X_1)$ or $f(X_2)$. Actually one element in the Reeb graph of a compact manifold represents all points having the same value under a real function. Figure 1 illustrates an example of a Reeb graph for a torus (a). The function f is the "height" function which here simply returns the value of the coordinate z of a point X. The corresponding Reeb graph is shown in (b) where the branches represent the isovalued and connected points. Critical points are represented by nodes that mark the ends of the branches. Triangular nodes denote local extrema points and square nodes denote saddle points. By applying Reeb Graph to a human figure, we can get a skeletal representation as illustrated in Figure 1, where the height function is adopted. It can be noticed that the critical points have important meanings on the skeletal figure. Extrema points represent head top, hand tips and foot toes. Saddle points represent armpits and groin. Moreover, the branches in the graph reflect the body parts of the figure, i.e., arms, legs, torso and head. Therefore by detecting branches, we can obtain the data corresponding approximately to the body parts of the human figure. This is the key idea behind our approach.

2.1 Discrete Reeb Graph

The classical Morse theory is concerned with only non-degenerate critical points of smooth functions (Morse function) on smooth manifolds. In practice, our data format does not comply with this assumption. The data consists of points sampled on the measured HB surface. The data might be corrupted by noise and gaps. The construction of the Reeb-Graph for such data, is inspired from the approach of Biasotti *et al* [12,13] who proposed an Extended Reeb Graph which can be extracted from discrete surface, where the data is described with a set of polygonal contours. In our case the data is an unorganized cloud of 3D data points. We call the Reeb graph extracted from such data the Discrete Reeb Graph (DRG). The extraction is based on the notion of connectivity described in the following definitions:

Defenition2 (connectivity of point sets): *Two point sets* $P = \{p_i\},\ i = 1..m$ *and* $Q = \{q_j\},\ j = 1..n$ *are defined as connected if* $\exists\, p_i \in P$ *and* $q_j \in Q$ *such that* $|p_i - q_j| \leq d$.

Where $|p_i - q_j|$ means the distance between points p_i and q_i and d is a threshold that denotes the maximum distance between a pair of connected points. The above definition also holds for the connectivity between two points for the particular case where the sets P and Q contain a single point each.

Definition 3 (connective point set): *A point set* C *is connective if* $\forall$ *subset* $\Omega \subset C$ *and* $\Omega \neq \emptyset$, Ω *and* $\bar{\Omega}$ *are connected.* Where $\bar{\Omega}$ is the complement of Ω in C.

Based on the above definitions the DRG is built on the discrete set of points according to the following steps:

Step1:Establishing level-set curves

For a continuous surface, a level-set curve is the intersection between a plane of a certain height and the surface. Due to the discrete nature of data, we extract data in a slice with a height in the domain $[h, h + l]$, where h is a height value and l is the slice thickness. By choosing an appropriate value of l, each slice will contain sufficient number of data points for the analysis to succeed. The data is sliced from bottom to top. In all, there are $ceil(\frac{h_{max}-h_{min}}{l})$ slices. Here $ceil()$ represents the nearest integer towards positive infinity and h_{max}, h_{min} denote the maximum and minimum height value of the data. For each slice, data points are grouped into several discrete connective sets consisting of connected data points based on the definition of connectivity above. These groups which we call discrete curves represent the level-set curves in the DRG.

Step2: Building the connectivity graph

Considering each curve as a node in the graph, two nodes in two adjacent slices respectively are linked if their corresponding curves are connected. In this way, we can build up a graph containing all nodes and their links, i.e., DRG.

Note In the DRG, critical points might degenerate to "critical curves". In other words, we might not discover the exact critical points due to the discreteness of data and the slicing process, instead these points appear to be critical curves around which the topology of HB varies. Therefore we do not distinguish critical points and critical curves in our application, and generally we denote them 'critical nodes' in the DRG.

3 The segmentation algorithm

Before presenting the details of the segmentation algorithm, we describe our problem in a precise manner. First of all, the subject of our study is a general human figure. The data is acquired by a general 3D scanner, and no prerequisites are placed on the specification the scanner. The data might be corrupted with noise, holes and gaps. Moreover, the human figure stands in the measuring platform with arms held at the sides and legs separated. Therefore the height direction of the measured figure is known. In order to segment scan data according to the DRG, we need firstly to extract critical nodes in the DRG, and then locate branches representing body parts, finally we retrieve the data points corresponding to the branches.

Finding critical nodes in the classical Reeb Graph is very intuitive. The root and leave nodes represent local extrema points. The branched nodes represent saddle points. However, it is nontrivial to extract critical nodes in DRG, because the noise and holes might change the local topological properties of the scan data and create 'false' critical nodes. This problem has been tackled as follows, first we established three primary topological patterns that appear in the DRG. These patterns are called O-type, λ-type and Y-type (Figure 2). O-type has two saddle nodes connected by two

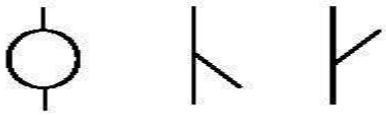

O-type, λ-type Y-type

Figure 2. Three main patterns in the DRG.

branches. λ-type has only one saddle node with a leave branch downward. Y-type is similar to λ-type, but has a leave branch upward.

Assuming that the HB posture is reasonably close to the standard posture shown in Figure 1, an ideal Reeb Graph should comprise a tree structure containing only λ-type patterns. The O-types and Y-types that appear in the real case reflect therefore holes and gaps in the data and must be discarded. However holes in the data might also generate the

λ-type pattern in the DRG. The detection of the related false nodes in such cases is based on the assumption that the size of a 'false' branch in λ-type caused by holes is quite small compared to the size of the whole body structure. This assumption is valid because a hole in the data has a very limited area compared to the overall HB surface, otherwise the data set itself would not represent a viable HB scan.

Based on these considerations, the following criteria are then proposed to identify 'true' critical nodes in DRG:

- A "true" saddle node has at least two "true" branches all of which are long enough (greater than a threshold).
- "True" extrema nodes are the deepest leaves of "true" branches

The segmentation algorithm is based on the analysis of the DRG and the above criteria. The algorithm contains only one pass searching from the bottom to the top of data. In this pass, the critical nodes representing foot toes, groin, hand tips, armpits and head top are detected using the criteria mentioned above, and the 'true' branches between these critical nodes are extracted. Then the identification of branches corresponding to the body parts becomes very simple. The branches between the groin and foot/toes correspond to legs and the branches between armpits and hand tips correspond to arms. The reminder of the data corresponds to torso and head. The algorithm for building the DRG and finding the 'true' saddle nodes and branches is described by the following pseudo-code

Notation

Node: A node is an entity which contains a curve in a slice.
NewNode(): A function to allocate a new node.
Class: A class is defined as a group of connected nodes.
Class(Node): The Class containing the Node.
NewClass(): A function allocating a new class
Num(Class): The number of nodes in the class
Threshold: Threshold is the number of nodes in a class, above which the class is considered as a "true" branch
Branch: The 'true' branch connected to a 'true' saddle node.

Code:

Slicing from bottom to top
For each slice
  Group data points into curves
  For each curve
    node:=NewNode()
    If it is the 1-st slice
      Class(node) := NewClass()
    Else
      Find out the nodes $(N_1, N_2, .., N_m)$in the last slice connected to the node
      If m = 0
        Class(node):=NewClass
      Else
        $C := (Class(N_i) \bigcup Class(N_2)... \bigcup Class(N_m))$
        select the classes verifying:
        $\{C_i | Num(C_i) \leq Threshold,$
        $i = 1, 2, ., n,\ (n \leq m)\}$
        If $n \geq 2$
          For each C_i
            $Branch_j = C_i, j := j + 1$
            Remove C_i
          End For
        Else
          $Class(node) = \{N_1, N_2, ...N_m\}$
        End If
      End If
    End If
  End for
End for

4 Experiments

A series of experiments were conducted to test the validity of the approach. These experiments aim to evaluate the effectiveness of the algorithm in terms of quality of the segmentation and also to assess its robustness and stability with respect to: 1)Variation of the HB shape, scan source, and severely corrupted scan data. 2) Variation of the HB posture. 3)Variation of the HB scan reference.

4.1 Variation of the human body shape and scan source

The HB scans were collected from two different sources. The first is the Cyberware website [17], the second is the CAESAR project website [18]. In both sites, the scans were acquired by the Cyberware whole body scanner WB4[17]. This scanner uses laser-based technology in which a laser beam is projected on the body, the beam profile is captured by different cameras around the body. The data from each image are then combined to produce the 3D points of the body surface. The scanning time is around 17 seconds. Therefore the scan is subject to trimming effects. The set of collected scans contain 14 scans of different individuals including males and females. Each scan has contains a number of points around 13 000.

The second set of scans is collected by a Wicks&Wilson [19] HB scanner at the Edinburgh Virtual Reality Center [20]. This scanner is based on a Moire technology where fringe patterns, projected on the body, are captured by eight cameras (in fact four cameras are employed and a moving mirror system, provides another 4 viewing positions). The set of 3D points extracted from each camera (triangulating with the fringe projector) are combined together to form the whole scan. The scanning time of this device is around 8

seconds, yet the person is required to stand very still during the scanning. The space inside the scanner is very limited and allows little freedom of the body movement. For these reasons, it was difficult to perform scans for a non-standard postures. We did managed however to obtain a few non-standard postures after many trials and collecting a set of 8 scans related to three different male individuals. The number of points in each scan is around 11 000.

Figure 3 shows the segmented cybeware HB scans. The first two rows show the scanned persons and their associated segmented scans. These scans were collected from the Cyberware [17]. The rest of the rows contain scans retrieved from the CAESER [18] website. The photographic images of the scanned persons are not available at that site. Results obtained with the second scan data set are illustrated in Figure 5, where the segmented scans are shown together with the images of the scanned persons, taken during the scanning process.

In the above figures, we can observe that scans of svelte persons, in a standard posture and having limbs well separated, are segmented with a reasonable accuracy(scans 1 to 6 in Figure 3 and 1,2,4,5, 6 and 7 in Figure 5. For these types of body profile, joints such as the groin and the armpit can be detected quite faithfully. For relatively stout persons, the segmentation is acceptable as long as the limbs are well separated (7 to 12 in Figure 3), when this is not the case, as in scans 13 to 15 , the segmentation is less faithful to the body anatomy. Segmentation errors are manifest, for instance, by parts of the legs and the arms being segmented as part of the torso. This result is as expected, because where the legs join, or the arms intersect with torso, result in connected data points which are then considered as part of a same homology group by the algorithm.

Scans 3 and 8 in Figure 5 correspond to a non-standard posture. By experimenting these postures, we aimed to test the behavior of the segmentation technique when the assumption of a standard posture is not respected. The segmented scans show that small region of the arms were segmented as part of the torso. This is explained by the fact that, for a given Morse function(the height function in our application), the location of the critical nodes (critical curves in DRG, which marks the borders between the branches) changes with the configuration of the posture. In posture 8, for instance, it is the left elbow that represents a location of critical curve rather than the left armpit.

Nevertheless for both groups of scans, the segmentation always results in five distinct components, even for the non-standard postures. Furthermore the partitioning is faithful to the HB anatomy in the sense that each segmented region belongs to a distinct body component.

It is also worth mentioning that these results were obtained with poor scan data as illustrated in Figure 4(a) which shows a zoomed area around the groin. The non-regular

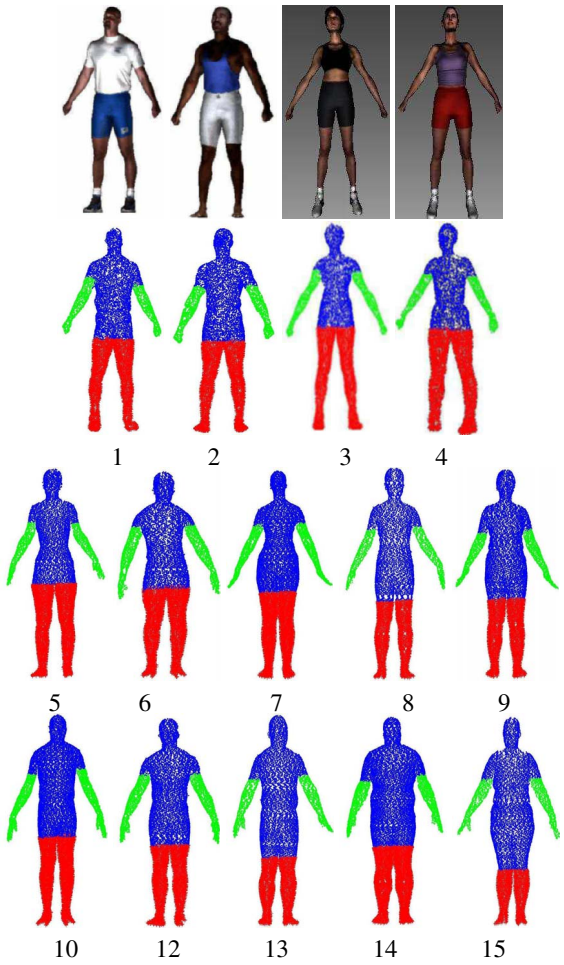

Figure 3. Segmenttion of HB scans acquired from the Cyberware scanner.

sampling of the data and the presence of gaps and holes are clearly visible. To test further the robustness of the algorithm, we corrupted the data by creating large holes in selected scans. The segmentation of these scans, shown in Figure 4(b) was not affected by the presence of holes, despite their large size. These results confirm that the algorithm is capable of discarding effectively the O type critical nodes (critical curves) described in Section 3.

4.2 Variation of the human body posture

The folowing experiments aim to test the stability of the algorithm with respect to posture variation. Naturally the algorithm is not expected to segment any arbitrary posture since the approach was built on the assumption that the HB

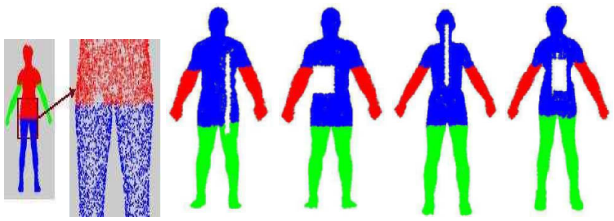

(a) (b)

Figure 4. (a) Zoomed image illustrating the distribution of the scan data. (b) Segmented HB scans corrupted by large holes.

pose is reasonably close to the standard pose. Nevertheless it is desirable that the algorithm should be able to cope with moderate variations around the standard posture. The set of varied postures was obtained as follows: A parameterized human skeleton template was coupled to a Cyberware HB scan. Then sets of random parameters values, centered at the values associated to the standard posture, were generated. Each set was then applied to the template to generate instances of the HB model. A set of artificial scans representing a variety of HB postures could then be obtained. The segmentation results are shown in Figure 6. All the scans were segmented into five parts and retained reasonable fidelity to the structure of HB anatomy. The locations of the armpits and the groin vary slightly in the segmented scans. This illustrates the stability of the algorithm with respect to moderate variations, and confirms that the algorithm generates a fair segmentation as long as the geometric configuration of the posture remain close to the skeletal representation of Figure 2.

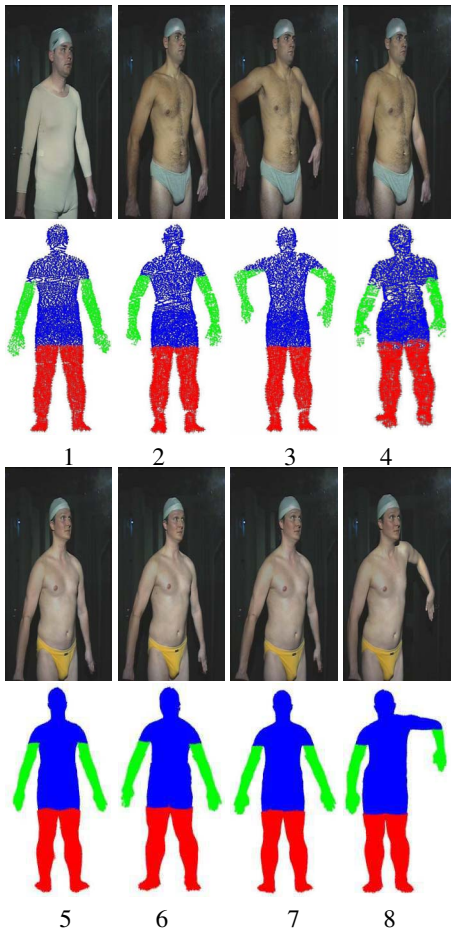

Figure 5. Segmenttion of HB scans acquired from the Wick&Wilson scanner.

4.3 Variation of the human body scan reference

The choice of the height function, used in the construction of the DRG, requires the principal orientation of the body to be co-aligned with the **z** axis of the coordinate reference attached to the HB scan. This condition cannot be satisfied exactly for many reasons, such as the presence of systematic errors in the scan data or the inevitable imperfections in the posture assumed by the scanned person. A series of experiments were conducted to check the behavior of the algorithm in such cases. These effects were simulated by applying rotations on some scans, around the axes **x** and **y** of the coordinate reference. The angles of rotations comprised: -30^o, -20^o, -10^o, 10^o, 20^o, and 30^o. The segmented scans are shown in Figure 7. Each row corresponds to a different person. Scans rotated around the **x** axis are in rows 1 and 2 and those rotated around the **y** are in rows 3 and 4. From the figure it is evident that the changes that affected the critical curves in terms of location and orientation, reflect the characteristics of the rotations. For instance , it can be observed that for the scans in the two last rows, the orientation of critical curve at the level of the groin is biased towards the angle of the rotation applied on the scan. This aspect is less visible in the scans rotated around the **x** axis because the scans are shown from the front view of the body, which direction is collinear to the **x** axis. The changes at the locations of the armpits and the groin can be observed though.

The results show that moderate perturbations on the orientation of the scan, e.g. less than 10^0 can be tolerated. Perturbations of large amplitude perturbation affect the quality of the segmentation, however the topological properties of the HB template remain preserved.

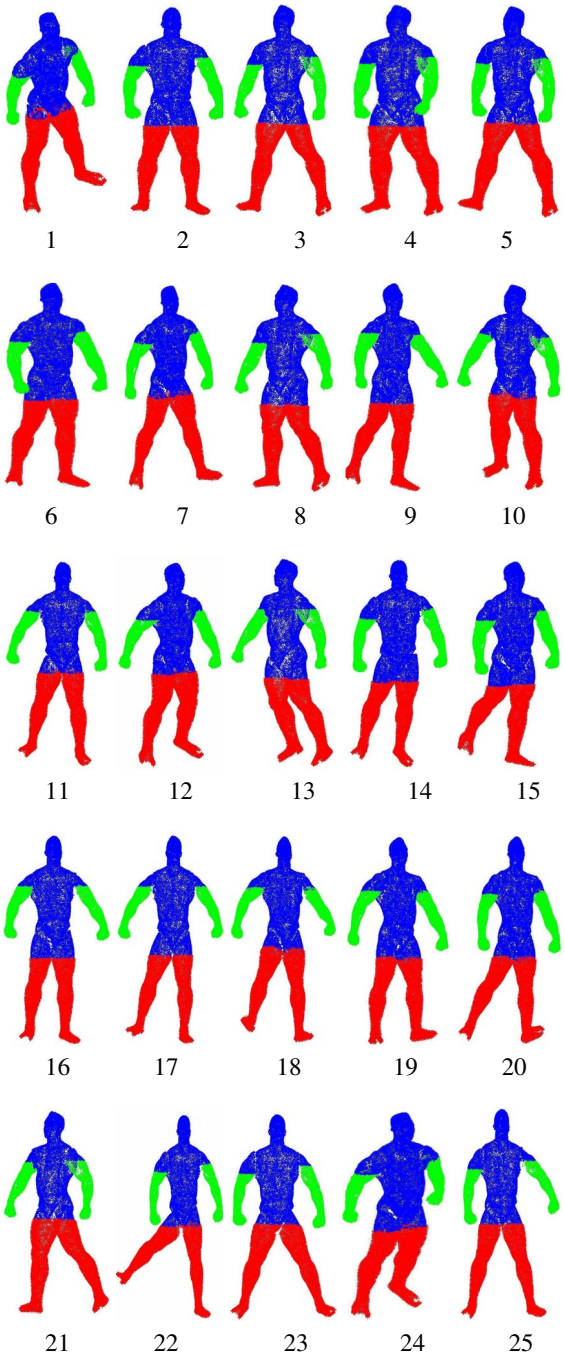

Figure 6. Segmentation of a set of animated HB scans.

5 Conclusion

This paper presents a new approach for the segmentation of HB scans based on topological analysis. The approach extends the Reeb graph framework to deal with unorganized cloud of data points by defining and utilizing connectivity concepts. With respect to previous works, our approach is differentiated by the following aspects: 1) It handles directly the raw scan data without the need of any preprocessing or pre-formatting stages. 2) It involves only topology-based techniques 3) The approach is implemented in a single pass algorithm, no post-processing is involved.

We validated our approach by conducting segmentation experiments using data collected from different types of HB scanners, containing scans covering a variety of HB shapes and profiles and including some severely damaged scans. The results confirm the robustness of the algorithm with respect to the diversity of scan sources, diversity of the body shapes and the poorness and corruption of the scan data.

From a quantitative point of view , the experiments confirm the reliability and the repeatability of the algorithm. In the 72 segmentation trials shown in this paper, the algorithm always segmented the scan into 5 connected and compact parts that respect the topology of the HB. For example, cases of under-segmentation, over-segmentation, or cases where a segmented part contains disjoint subparts (e.g. from the arm and the leg), never occurred.

From a qualitative point of view , if we disregard pathological postures that violate severely our pose configuration assumption, the algorithm produces a reasonably faithful segmentation of the HB anatomy. Contrary to previous approaches, our approach proves to be capable of handling moderate variations around the standard posture, either at the level of the whole scan orientation or at the level of posture configuration.

Being based on topological analysis, the approach is intrinsically not qualified to handle postures where limbs are joined together, for example closed legs, or arms touching the torso. To be able to deal with such cases requires that the contours of discontinuities between the joined parts of the body be detected and labelled explicitly perhaps based on local surface analysis and differential geometry techniques. The work developed in [21], for example, could perhaps afford an appropriate framework for handling the above cases.

The next stage of this work will be the extension of the algorithm so that it can accommodate a larger range of postures. We are currently investigating an approach that builds a set of complementary Reeb-Graphs associated to appropriate generic functions and hereafter analyzing the resulting critical curves while integrating the geometrical constraints on the HB posture.

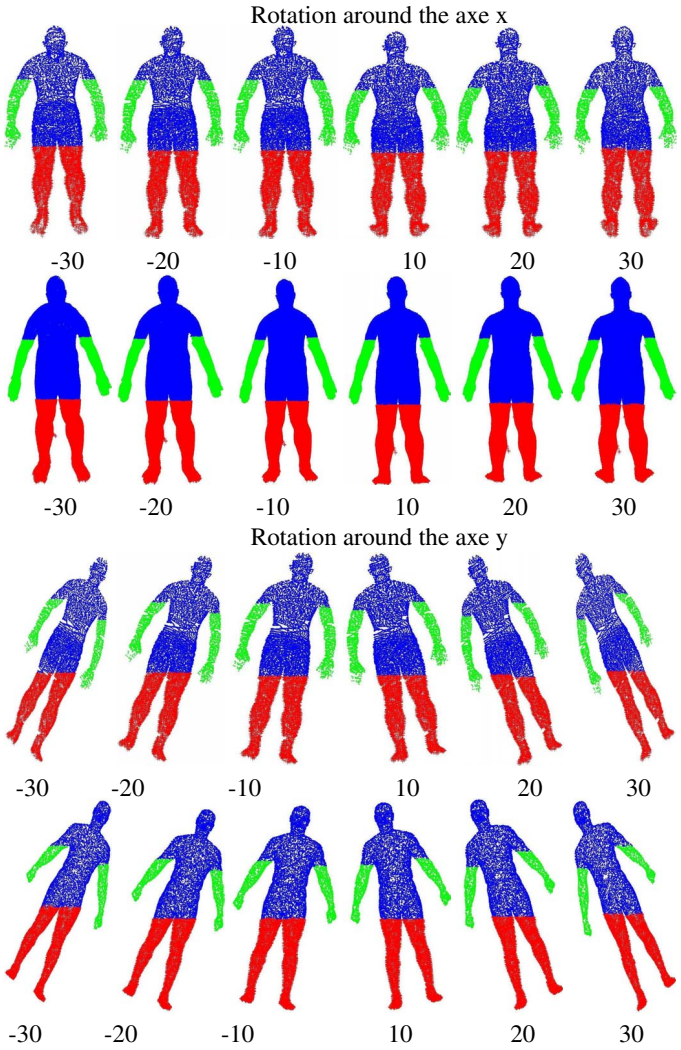

Figure 7. Segmentation of rotated scans.

Acknowledgement

This work is supported by an EPSRC Grant Ref:R0538

References

[1] P.R.M. Jones, M. Rioux, "Three dimensional surface anthropometry:applications to human body", Optics and Lasers in Engineering, Vol. 28, No. 2, pp.89- 117, 1997.

[2] E. Paquet, K.M Robinette, M. Rioux, "Management of three-dimensional and anthropometric databases: Alexandria and Cleopatra". J. Electronic Imaging, Vol. 9, pp. 421-431, 2000.

[3] R.P. Pargas, N.J. Staples, J.S. Davis, "Automatic measurement extraction for apparel from a three-dimensional body scan", Optics and Lasers in Engineering, Vol. 28, No. 2, pp.157-172, 1997.

[4] D. Protopsaltou *et al*, " A body and Garment Creation Method for an Internet-Based Virtual Fitting Room", Advances in Modeling, Animation and Rendering, J. Vince and R.Earnshaw eds, pp.105-122, Springer-Verlag.

[5] F. Cordier, H. Seo, N. Magnenat-Thalmann, "Made-to-Measure Technologies for an Online Clothing Store", Computer Graphics and Applications, pp.38-48, Jan-Feb 2003.

[6] J. Starck *et al*, "Animated statues", Journal of Machine Vision Applications, 2002.

[7] M. Lin, "Tracking Articulated Objects in Real-Time Image Sequences", Proc. International Conference on Computer Vision, pp.648-653, Corfu, Greece, 1999.

[8] J.H. Nurre, "Locating landmarks on human body scan data" Proc. Conf. 3D Digital Imaging and Modeling, pp.289-295, Ottawa, Canada, 1997.

[9] X. Ju, N. Werghi, and J. P. Siebert, "Automatic Segmentation of 3D Human Body Scans", Proc. Int. Conf. on Computer Graphics and Imaging 2000 Las Vegas, USA, 2000.

[10] L. Dekker I. Douros B. F. Buxton P. Treleaven, "Building Symbolic Information for 3D Human Body Modeling from Range Data", Proc. Conf. 3D Digital Imaging and Modeling, , pp. 388-397, Ottawa, Canada, 1999.

[11] I. Douros, L. Dekker, B. Buxton, "Reconstruction of the surface of the human body from 3D scanner data using B-splines", Proc. SPIE vol. 3640, pp234-245, San Jose, California, January 1999.

[12] C.L Wang, T.K, Chang, M. Yuen, "From laser-scanned to feature human model: a system based on fuzzy logic concepet", CAD, Vol.35, pp. 241-253, 2003.

[13] M. Hilaga, Y. Shinagawa, T. Kohmura, T. .Kunii, "Topology matching for fully automatic similarity estimation of 3d shape". SIGGRAPH 2001, pp 203 -212, New York, USA.

[14] Y. Shinagawa, T.L. Kunii and Y.L. Kergosien. "Surface Coding Based on Morse Theory" , IEEE Computer Graphics and Applications, Vol.11, No.5, pp.66-78, 1991.

[15] S. Biasotti, M. Mortara, M., M. Spagnuolo, "Surface Compression and Reconstruction using Reeb graphs and Shape Analysis, Proc. of Spring Conference on Computer Graphics, pp. 175-184, Bratislava 2000.

[16] S. Biasotti, B. Falcidieno, M. Spagnuolo, "Extended Reeb Graph for Surface Understanding and Description", G.Borgefors, I. Nystm, G. Sanniti di Baja (eds) Lectures notes in Computer Sciences, pp. 185-197, 2000

[17] Cyberware, www.cyberware.com

[18] Civilian American and European Surface Anthropometry Resource, http://www.hec.afrl.af.mil/cardlab/caesar/

[19] Wicks and Wilson, http://www.wwl.co.uk/wwl2/index.html

[20] EDVEC: http://www.edvec.ed.ac.uk

[21] F. Ferrie, J. Lagharde, P. Whaite, "Darboux Frame, Snakes and Super Quadrics, Geometry from the Bottom Up", IEEE Trand. PAMI, Vol.15, No.8, 1993.